Clinical Biomechanics 52 (2018) 33–40

Contents lists available at ScienceDirect

Clinical Biomechanics

journal homepage: www.elsevier.com/locate/clinbiomech

De novo generation in an *in vivo* rat model and biomechanical characterization of autologous transplants for ligament and tendon reconstruction

Marc Soubeyrand[a,b,f], Elisabeth Laemmel[b], Nathalie Maurel[c], Amadou Diop[c,*], Thierry Lazure[d], Jacques Duranteau[b,e], Eric Vicaut[b]

[a] Department of Orthopaedic Surgery, Bicetre Universitary Hospital, Public Assistance of Paris Hospital, France
[b] Laboratoire d'Etude de la Microcirculation, Faculté de Médecine Diderot Paris VII, U942, Paris, France
[c] Equipe Biomécanique et Remodelage Osseux, Ecole Nationale Supérieure d'Arts et Métiers, 151 Boulevard de l'Hôpital, 75013 Paris, France
[d] Department of Pathology, Bicetre Universitary Hospital, Public Assistance of Paris Hospital, France
[e] Department of Intensive Care and Anesthesiology, Bicetre Universitary Hospital, Public Assistance of Paris Hospital, France
[f] Faculty of Medicine, University Paris Sud-XI, 63 rue Gabiel Peri, 94270 Le Kremlin-Bicêtre, France

ARTICLE INFO

Keywords:
Tissue bioengineering
Rat model
Ligament
Tendon
Reconstructive surgery
Biomechanics

ABSTRACT

Background: Surgical reconstruction of ligaments and tendons is frequently required in clinical practice. The commonly used autografts, allografts, or synthetic transplants present limitations in terms of availability, biocompatibility, cost, and mechanical properties that tissue bioengineering aims to overcome. It classically combines an exogenous extracellular matrix with cells, but this approach remains complex and expensive. Using a rat model, we tested a new bioengineering strategy for the *in vivo* and *de novo* generation of autologous grafts without the addition of extracellular matrix or cells, and analyzed their biomechanical and structural properties.
Methods: A silicone perforated tubular implant (PTI) was designed and implanted in the spine of male Wistar rats to generate neo-transplants. The tensile load to failure, stiffness, Young modulus, and ultrastructure of the generated tissue were determined at 6 and 12 weeks after surgery. The feasibility of using the transplant that was generated in the spine as an autograft for reconstruction of medial collateral ligaments (MCL) and Achilles tendons was also tested.
Findings: Use of the PTI resulted in *de novo* transplant generation. Their median load to failure and Young modulus increased between 6 and 12 weeks (respectively 12 N vs 34 N and 48 MPa vs 178 MPa). At 12 weeks, the neo-transplants exhibited collagen bundles (mainly type III) parallel to their longitudinal axis and elongated fibroblasts. Six weeks after their transfer to replace the MCL or the Achilles tendon, the transplants were still present, with their ends healed at their insertion point.
Interpretation: This animal study is a first step in the design and validation of a new bioengineering strategy to develop autologous transplants for ligament and tendon reconstructions.

1. Introduction

The pathology of ligaments, referred to as sprains and articular instability, and tendinous ruptures are important concerns (Rodrigues et al., 2013), and surgical reconstructions are often needed to prevent disabilities. In most cases, these reconstructions are performed using autotransplants, allografts, or synthetic transplants (Cheng et al., 2014; Ng et al., 2013). However, these options can be complicated by several issues including availability, inherent complications of the harvesting procedure for autografts, infectious hazard for allografts, and wear or inflammatory reactions for synthetic transplants (Chen et al., 2009). Tissue bioengineering aims to overcome these limitations, typically by combining an exogenous extracellular matrix (ECM) – or scaffold – with cells either directly *in vivo*, or *in vitro* using bioreactors. However, this approach remains expensive and complex (Abousleiman et al., 2009; Chen et al., 2009; Thorfinn et al., 2012). To circumvent these difficulties, we devised a new strategy for *in vivo* bioengineering. Our strategy aims to generate autologous neo-transplants without the addition of cells or ECM (*i.e. de novo* generation). It consists of using a silicone perforated tubular implant (PTI) to guide the tissue generation process.

Previous studies involving *in vivo* implantation of silicone tubes

* Corresponding author.
E-mail address: amadou.diop@ensam.eu (A. Diop).

https://doi.org/10.1016/j.clinbiomech.2017.12.006
Received 9 May 2017; Accepted 12 December 2017

demonstrated that they induced formation of vascular grafts (Chen et al., 2013; Hallin and Sweetman, 1976). However, these tubes were not subjected to repetitive uniaxial stresses because they were simply deposited in the body. It is well established that this type of stress is important for healing tendons and ligaments and for guiding and stimulating the *in vitro* migration of fibroblasts (Abousleiman et al., 2009; Altman et al., 2002; Doroski et al., 2010; Issa et al., 2011). We therefore hypothesized that if the silicone tube was exposed to this type of stress, it would be able to guide the fibroblasts and generate a neo-tissue resembling a tendon or ligament. For this purpose, we chose to attach the ends of the tube to bone surfaces that are physiologically mobile in relation to each other.

The PTI, which was used as a guide and not as a scaffold, was initially empty but allows the body's fluids and cells to circulate after surgery. We expected that, at the end of the process, the PTI would be filled with a new tissue, which could be harvested and potentially used as a transplant in ligament and tendon reconstructive surgery.

The objective of the present study was to test the feasibility of this strategy in rats before any evaluation in humans. The first goal was to validate the hypothesis that the healing process can be guided to generate *de novo* a neo-transplant using this PTI procedure in a rat spinal model. The second aim was to analyze the mechanical and ultrastructural characteristics of the ~~thus~~ generated transplant at different time points in the healing process. Finally, we carried out preliminary attempts at transferring such a transplant to the knee or the calf for medial collateral ligament (MCL) or Achilles tendon reconstruction.

2. Methods

Male Wistar rats (body weight: 300–400 g, 7–9 weeks, Janvier company, Paris, France) were used in the study. An Institutional Animal Care and Use Committee approved the study (Bioethics committee for animal experiments, Lariboisière Faculty of Medecine, Paris).

2.1. Manufacture and features of the perforated tubular implant (PTI)

A silicone tube (Mono-lumen tubing, Helix Medical, inner diameter of 3.35 mm, outer diameter of 4.65 mm) was cut at a length of 40 mm.

We used silicone as it can support the adhesion of fibroblasts and promote their migration (Brunette, 1986; Mirzadeh et al., 2003). During preliminary experiments, we tested several configurations (number and size of the holes, position of the holes, thickness of the tube wall, *etc.*); subsequently we selected the configuration used in the present study.

A stainless-steel tube 2.98 mm in diameter was then used as a punch to pierce a total of 14 holes arranged in staggered rows (Fig. 1a). The geometry of seven PTI was assessed using a desktop Micro-CT (Skyscan 1176; Bruker microCT, Kontich, Belgium): the mean diameter of the holes was 2.59 mm (SD 0.01 mm) and the mean distance between two successive holes was 7.39 mm (SD 0.004 mm). The stiffness of these seven PTI was quantified using a tensile test (Instron 5565 model, Norwood, MA) and the mean value was 0.47 N/mm (SD 0.04 N/mm).

2.2. Design of the study

Different groups of rats were analyzed to address the different aims of the study.

A first group of 19 rats underwent implantation of the PTI in the spine (see below for the procedure) and were sacrificed at 6 weeks (n = 10) or at 12 weeks (n = 9) after implantation. After opening the PTI, the generated neo-transplants were harvested for biomechanical testing (n = 7 at 6 weeks and n = 6 at 12 weeks) and histological examination (n = 3 at 6 weeks and n = 3 at 12 weeks).

To determine whether the PTI was necessary for generating a neo-transplant, the same surgical procedure was performed in a control group (n = 6) without implanting any implant. Similarly, to determine whether perforation of the implant wall was necessary, we implanted a tubular implant devoid of holes in another group (n = 6). Rats were sacrificed at 6 weeks for these two groups.

In a final group (n = 4), we tested the feasibility of the use of the neo-transplant generated in the spine as an autograft for the reconstruction of ligaments and tendons in other joints; in this case, either the MCL (n = 2) or Achilles tendon (n = 2). These small sample sizes were due to the fact that in this group we simply aimed to determine whether the neo-transplant generated in spine could be used as an autograft. Animals were first implanted with a PTI in the spine for 6 weeks to generate the transplant, and underwent a second surgery for transfer of the neo-transplant to the knee or the calf (see below for procedure). They were sacrificed 6 weeks after this second surgery and the reconstructed joint was harvested for macroscopic and histological examination.

2.3. Surgical procedure

2.3.1. General aspects

For all surgeries, rats were anesthetized with 2.5% isoflurane in balanced oxygen, and buprenorphine (50 μg/kg) was injected subcutaneously 20 min prior to surgery. Before incision, skin was shaved and prepared with an antiseptic solution (Betadine, Melda, Solna, Sweden). For non-terminal surgeries, the postoperative pain was controlled with buprenorphine (50 μg/kg/12 h) for 3 days and prophylactic antibiotic treatment (Amoxicillin 1 g/L + Clavulanic Acid 125 mg/L) was administered orally through the water bottle for 2 days. For terminal surgeries, rats were sacrificed with an overdose of isoflurane and the transplants generated in the tubular implants were harvested.

2.3.2. Implantation of the perforated tubular implant in the spine (Fig. 1b)

A 5-cm midline incision was performed at the lumbar spine level and spinous processes were exposed from the second lumbar vertebra (L2) to the sixth vertebra (L6).

The spine was chosen because of the ease of access *via* a posterior approach, and because the large size of the spine (relative to the animal's size) allows for the use of larger implants for the generation of larger neo-transplants (which are therefore easier to characterize).

The spinous processes of the third, fourth, and fifth lumbar vertebrae (L3, L4, L5) were then removed in order to provide a space for the tubular implant. Before implantation, the PTI was dipped into a bath of antiseptic solution (Anios'clean Excel D, Anios) for 15 min and then rinsed with sterile saline. The implant was sutured to the spinous processes of L2 and L6 with a 4/0 Prolene suture. The suture was passed through the wall of the PTI and through the interspinous ligament between L6 and the sacrum before the knot was tightened. The dorsal aponeurosis and the skin were closed. We chose to suture the ends of the PTI to the spinous processes because we wanted to apply cyclic constraints to the neo-transplant that was growing in the tube. Indeed, during physiological motions of the spine, all spinous processes move repeatedly in relation to each other.

2.3.3. Transfer of the neo-transplant for reconstruction of ligaments and tendons

We first implanted the PTI in the spine as described above. After 6 weeks, the rats were re-anesthetized to harvest the neo-transplant generated in the spine and the skin was closed. We then tested the feasibility of their use as a transplant for ligament or tendon reconstruction. We chose the MCL and the Achilles tendon because they are the biggest and the most accessible ones.

For the rats in which a MCL reconstruction was performed, the right knee was approached through a median anterior incision and the MCL was exposed. Tunnels were made in the femur and the tibia with a 1.2 mm drill bit at the level of the MCL insertions. The MCL was completely removed. The ends of the transplant were inserted into the

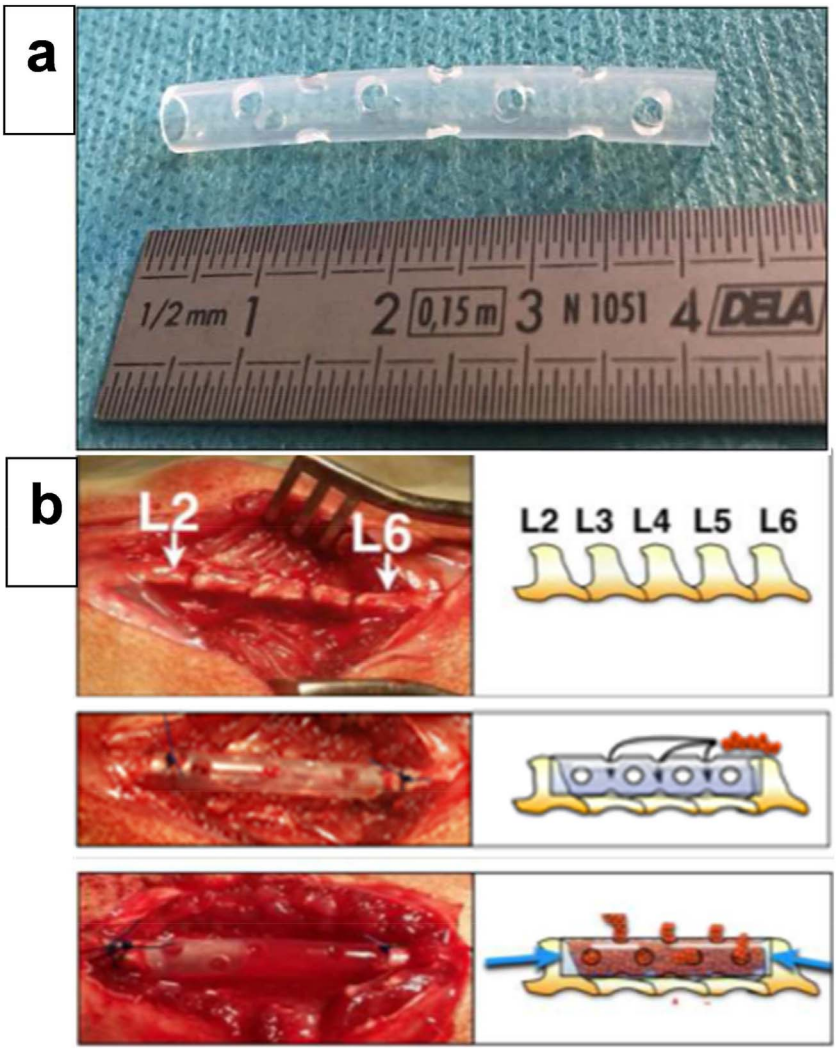

Fig. 1. (a) Global view of the perforated tubular implant. (b) Surgical technique for the implantation of the perforated tubular implant into the spine.

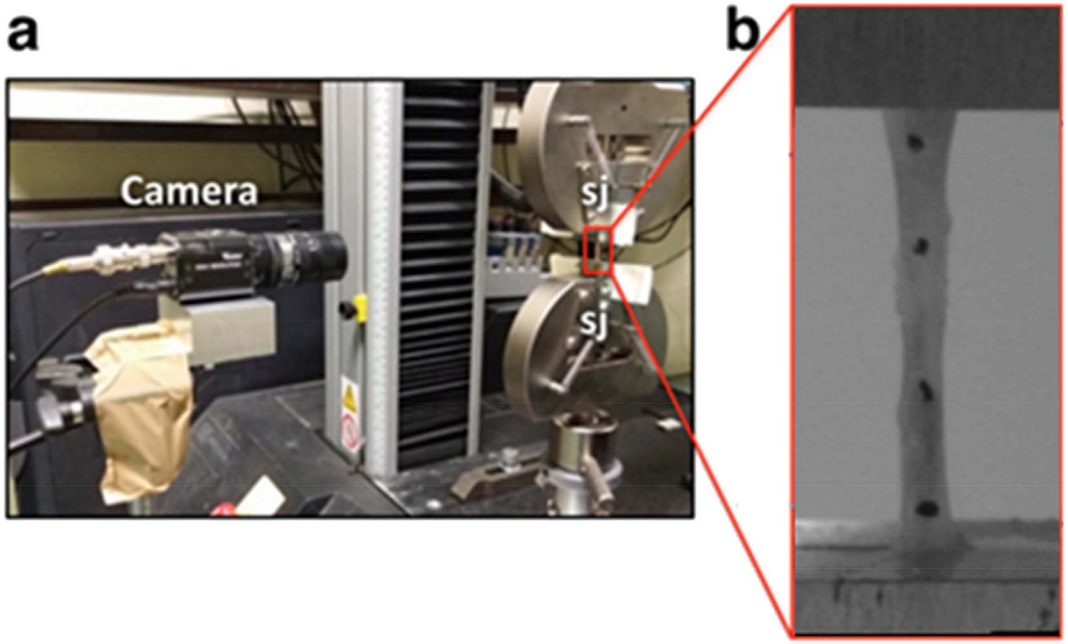

Fig. 2. Experimental protocol of biomechanical testing. (a) Global view of the tensile testing set-up. (b) Zoomed-in view of the neo-transplant fixed in striated jaws (sj) showing landmarks used for optical measurement of displacements (only the two most distal landmarks were analyzed here).

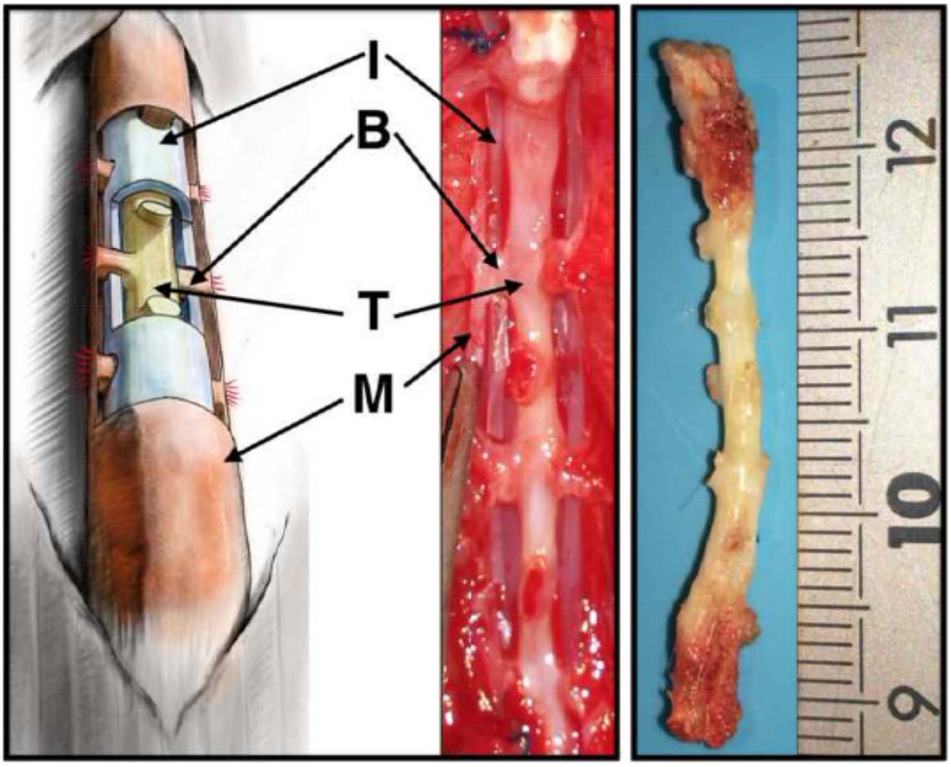

Fig. 3. Left: macroscopic aspect of the neo-transplant (T) in the perforated tubular implant (I) before harvesting. (M): membrane around the implant. (B): connecting bridges between the neo-transplant and the membrane. Right: neo-transplant isolated from the perforated tubular implant and the membrane.

femur and the tibia and fastened with a surgical knot of 4/0 Prolene. Muscles and skin were closed.

For Achilles tendon reconstructions, the left calf was approached through a median posterior incision and the Achilles tendon was exposed and removed. Its calcaneal insertion was decorticated with a scalpel blade to achieve a flat cancellous bone surface. A vertical 1 mm tunnel was made in the calcaneus through the site of the native insertion of the tendon. A 4/0 Prolene suture was successively passed in one end of the transplant and through the calcaneus to fasten the transplant to the calcaneus. The other end of the transplant was sutured with 4/0 Prolene to the belly of the triceps. Skin was closed.

2.4. Biomechanical characterization of the neo-transplant (Fig. 2)

At sacrifice, the neo-transplants were harvested and stored at − 20 °C in plastic wraps. They were thawed at room temperature just before mechanical tensile testing (Instron 5565 model, Norwood, MA). The two edges of the transplant were fixed in gauze using a cyanoacrylate base glue and were then placed between two layers of tape. The prepared specimen was finally fixed in striated jaws linked to the crossheads of the testing machine, with its longitudinal axis parallel to the loading direction. The initial length of the free part of the transplant between jaws was 15 mm. The tensile test was performed at a speed of 5 mm/min. The applied load was measured using a load cell with an accuracy of 0.1 N. The elongation of the specimen was optically measured using a CCD camera tracking the position of two mascara landmarks placed on it, with a pixel size of 0.09 mm. The two landmarks were 12.5 ± 1.3 mm apart to involve the maximum possible material in measurements and also to avoid disturbances due to the fixations in the jaws. The relative displacement between the two landmarks was computed using a custom-made software (Matlab) used in previous studies (Deranlot et al., 2014; Diop et al., 2011) and a load-displacement curve was obtained. A stress-strain curve was derived from this curve using the mean cross-sectional area of the sample and the initial distance between the two landmarks. The mean cross-sectional area was obtained measuring seven thicknesses on the first image before loading and assuming a circular section. Different parameters were defined from these curves. First, the load to failure was defined as the maximal load reached throughout the test. Second, the Young modulus was calculated by linear regression on a linear portion of the stress-strain curve. The extent of this portion was defined to maximize the coefficient of determination of the regression, which was always higher than or equal to 0.989. Its superior limit was set to the failure load or to a yield point occurring before failure (Fa). This yield point corresponded to the beginning of damage to the sample, leading to a disturbance to landmarks and subsequently to non-consistent strains and displacements. Finally, the stiffness of the sample was calculated as this yield load divided by the corresponding displacement. The load to failure, stiffness, and Young Modulus were compared at 6 and 12 weeks using a permutation test (Hothorn et al., 2008), with statistical significance set at $P < 0.05$.

2.5. Histological characterization of the neo-transplant

At sacrifice, the neo-transplants were harvested with their bony insertions. The neo-membrane surrounding the PTI was also harvested for histological characterization. The samples were fixed for 48 h in 10% neutral buffered formalin, decalcified (due to the presence of bony insertions) and embedded in paraffin. Transverse sections (4 μm) were obtained and placed on silanized slides for staining with HPS (hematoxylin phloxine saffron) and MT (Masson's trichrome). Immunohistochemical staining was carried out using hyaluronidase 0.5% for epitope recovery after deparaffinization. The slides were incubated overnight at 4 °C with the following anti-rabbit primary antibodies: type I collagen (1:2000), type II collagen (1:1000), and type III collagen (1:1000) (all from Novotec France). After inhibition of the endogenous peroxidases with hydrogen peroxide, slides were incubated for 45 min with the secondary antibody coupled to peroxidase (Dako). A reaction with diaminobenzidine (Dako) revealed the antigen/antibody complexes with brown staining.

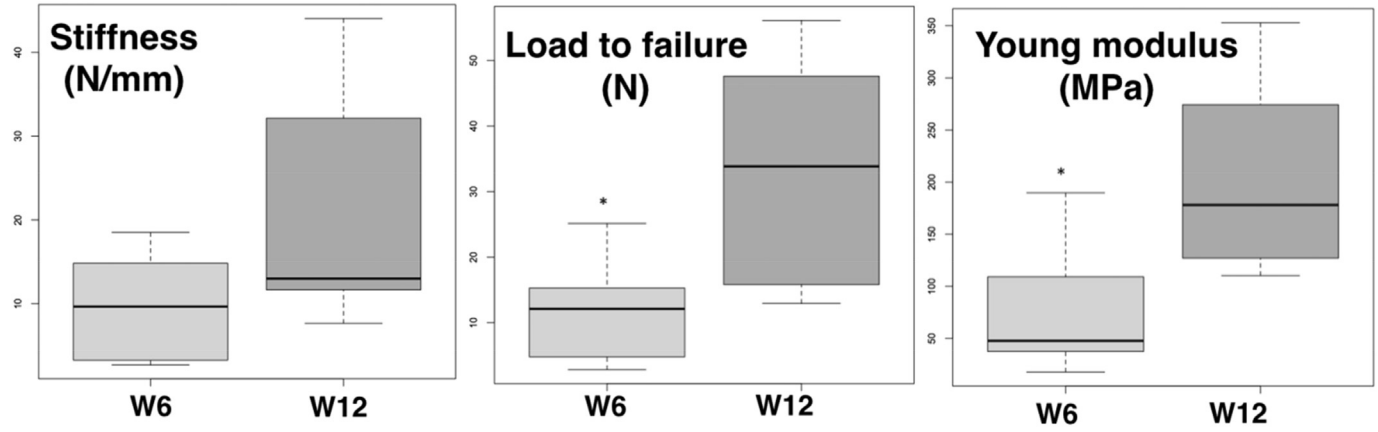

Fig. 4. Biomechanical tensile testing data, reported as median, interquartile range, minimal, and maximal values, as their distribution was not normal. * corresponds to $P < 0.05$.

3. Results

3.1. Generation of a neo-transplant

No tissue developed in any cases in the control group in which no implant was implanted (the paravertebral muscles simply healed on the medial line) or in the non-perforated tubular implant group. Conversely, following implantation of a perforated implant a new generated solid tissue was present in the implant (Fig. 3) at 6 weeks as well as at 12 weeks, indicating a dramatic effect of the presence of the PTI on *de novo* generation of this tissue. The neo-tissue was fixed to the spinous process of L2 and L6 and could be easily separated from the PTI. No inflammatory reactions occurred at the interface between the neo-tissue and the PTI. Connecting bridges passing through the holes of the PTI were present between the neo-tissue and the membrane that developed around the PTI. This membrane also developed around non-perforated tubes.

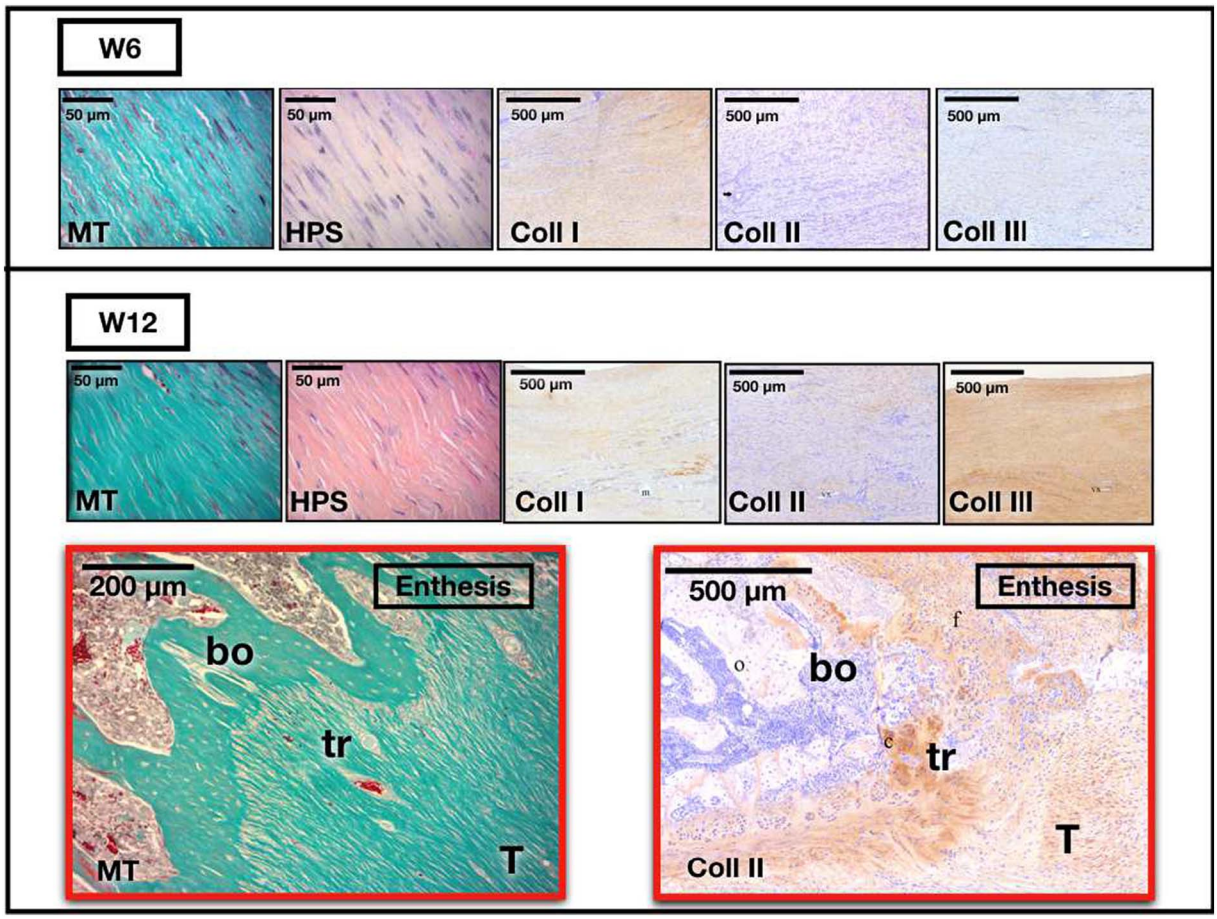

Fig. 5. Histological and immunohistochemical analysis of the neo-transplant at six (W6) and twelve (W12) weeks. Immunostaining reveals the corresponding collagen with brown color. The aspect of the enthesis developed between the neo-transplant and the bone is also shown at W12.
HPS: Hematoxylin phloxine saffron and MT: Masson's trichrome.
Coll I: Type I collagen; Coll II: Type II collagen; Coll III: Type III collagen. bo: Bone. tr: Transition zone. T: Neo-transplant. (For interpretation of the references to color in this figure legend, the reader is referred to the web version of this article.)

3.2. Biomechanical characterization of the neo-transplant (Fig. 4)

The median load to failure significantly increased from 12 N at 6 weeks to 34 N at 12 weeks ($P = 0.017$). Similarly, the median Young modulus significantly increased from 48 MPa to 178 MPa ($P = 0.012$). Median stiffness was 10 N/mm at 6 weeks and 13 N/mm at 12 weeks ($P = 0.1$).

3.3. Histological characterization of the neo-transplant (Fig. 5)

At 6 weeks, a vascular network with a global longitudinal orientation was visible alongside the collagen matrix of the neo-transplant. Immunostaining revealed a slight presence of type I collagen, while types II and III were not found.

At 12 weeks, the neo-transplant presented collagen bundles parallel to its longitudinal axis and elongated fibroblasts similar to tenocytes. Type III collagen formed the majority of these collagen bundles, while few fibers of types I and II collagen were observed. At the ends of the neo-transplant, we observed a classical aspect of enthesis, with three successive layers. The first layer corresponded to the neo-transplant, in which the collagen fibers were arranged parallel to longitudinally oriented fibroblasts. The second layer was a transition zone between the first and the third layer; immunostaining revealed the presence of type II collagen. The third layer was the bone. Dense layers of aligned fibroblasts made up the neo-membrane that developed around the PTI.

3.4. Transfer of the neo-transplant for reconstruction of ligaments and tendons

Six weeks after transfer, the neo-transplants were still present and had healed with the femurs and tibias in MCL reconstructions (Fig. 6a) or with the triceps surae and the calcaneus in Achilles tendon reconstructions (Fig. 6b). HPS and MT staining of longitudinal microsections of the neo-transplants revealed that collagen bundles remained longitudinally oriented with elongated fibroblasts.

4. Discussion

Here, we demonstrated using a rat model that it is possible to generate *in vivo* and *de novo* an autologous neo-transplant using only a perforated tubular implant to guide the physiological healing process.

Tissue bioengineering classically consists of the association of a scaffold – acting as an ECM – with seeded cells (Chen et al., 2009; Rodrigues et al., 2013; Yang et al., 2013). One limitation of this strategy is that the implanted cells are not always able to survive, multiply, or differentiate in the ECM. For example, various products made from synthetic or biological matrices are marketed to allow the reconstruction of tendons and ligaments (Chen et al., 2009). These products are initially devoid of cells and are supposed to be gradually colonized by the patient's cells. However, their ability to induce regeneration of ligament or tendon-like tissue remains limited. Fibroblasts must be able to colonize the matrix and the latter must gradually degrade so that the fibroblasts can make their own matrix. Abdousleiman et al. proposed filling an umbilical vein with a collagen matrix and implanting it with mesenchymal stem cells (MSCs) (Abousleiman et al., 2008). They observed that, when exposed to uniaxial cyclic stresses, MSCs differentiated into fibroblasts which secreted a matrix composed of collagen fibers oriented parallel to the stress. However, this strategy is complex and potentially expensive because it involves obtaining the vein, making the matrix, and cultivating the cells. The originality of our method is that is does not require the addition of any matrix or cells.

Given that, in our technique, it is the fibroblasts recruited by the organism themselves that generate their own matrix, the synergy between the ECM and the cells is optimal by definition. Another advantage of our approach is that the generated neo-transplant is totally autologous, thereby removing concerns about immune compatibility or infectious transmission.

In an *in vivo* study, Doroski et al. (2010) encapsulated MSCs in a hydrogel and cultured them for 21 days using a bioreactor. At this time point they found some collagen I and a limited presence of Type III collagen. However, they observed an upregulation of type III collagen expression. The authors hypothesized that type III collagen would have been observed in higher quantities if the culture had been extended for a longer period. Chen et al. (2013) found that after one month, type III collagen mainly made up the neo-tissue covering a silicone tube implanted in the subcutaneous tissue and the abdominal cavity. Type I collagen was rarely observed. The diversity of experimental protocols from one study to another makes it difficult to draw absolute conclusions about the types of collagen involved in fibroblast neo-tissue genesis. However, it seems that the expression of type I collagen precedes that of type III collagen, which becomes particularly important after about a month. However, this sequence is different from that observed during normal healing of tendons, where type III collagen is first deposited and then replaced by type I collagen (Sharma and Maffulli, 2006).

No neo-transplant was generated in animals operated without implantation of a PTI, indicating an important effect of this device on transplant generation. The aim of the PTI was to guide and optimize the physiological healing process. We observed the development of a membrane around the PTI, which can be compared to that described by Masquelet (Christou et al., 2014). It was functionally connected to the organism and constituted a biological chamber for the growing neo-tissue.

The mechanical behavior is an essential aspect in characterization of such transplants, as they will be required to transmit or to resist mechanical loads when used for ligament or tendon reconstruction. Because the transplants were growing, we compared their biomechanical properties at 6 and 12 weeks. The load to failure and the Young modulus were significantly increased at 12 weeks, indicating a maturation of the transplant between the two time points. The biomechanical properties obtained at 12 weeks were consistent with those previously described in literature for native rat MCL and Achilles tendons (the stiffness is difficult to compare to literature, as it directly depends on the length of the tested samples; in this case, the length was not similar). The load to failure of the neo-transplant (34 N) was slightly higher than those described in literature (Keller et al., 2013; Mammoto et al., 2008; Su et al., 2008) for native MCL (range: 19.5–32.5 N) but were within the lower range of those described in literature (Ahmed et al., 2012; Kaux et al., 2013; Keller et al., 2013; Monteiro et al., 2011; Nourissat et al., 2010; Suwalski et al., 2010; Teramoto and Luo, 2008; Vieira et al., 2015) for native Achilles tendons (range: 31.6–87.7 N). The neo-transplant exhibited a Young modulus that was somewhat lower (178 MPa) than values described for the MCL (range: 314–369 MPa) but was in the range described for the Achilles tendon (range: 70–537.2 MPa). Thus, from a purely biomechanical point of view, this neo-transplant could be used as an alternative in MCL or Achilles tendon reconstruction in rat. We demonstrated the feasibility of such replacements in a pilot series (n = 2 per group) by the successful integration of the neo-transplant to the knee and to the calf after its transfer to reconstruct the MCL and Achilles tendon. However, this encouraging result requires further study using larger sample sizes.

We found that the ultrastructure of the neo-transplant presented collagen bundles that were regularly and longitudinally oriented following the axis of the PTI. To explain this result, our hypothesis is that during maturation, the neo-transplant was submitted to cyclical axial loadings related to the physiological motions of the spine. Indeed, as the tubular implant was stretchable, it did not prevent relative motions between the L2 and L6 spinous processes to which it was fastened, and therefore allowed the transmission of loads to the transplant inside. This hypothesis is supported by *in vitro* experiments showing that fibroblasts subjected to a repetitive uniaxial stress secrete a collagen

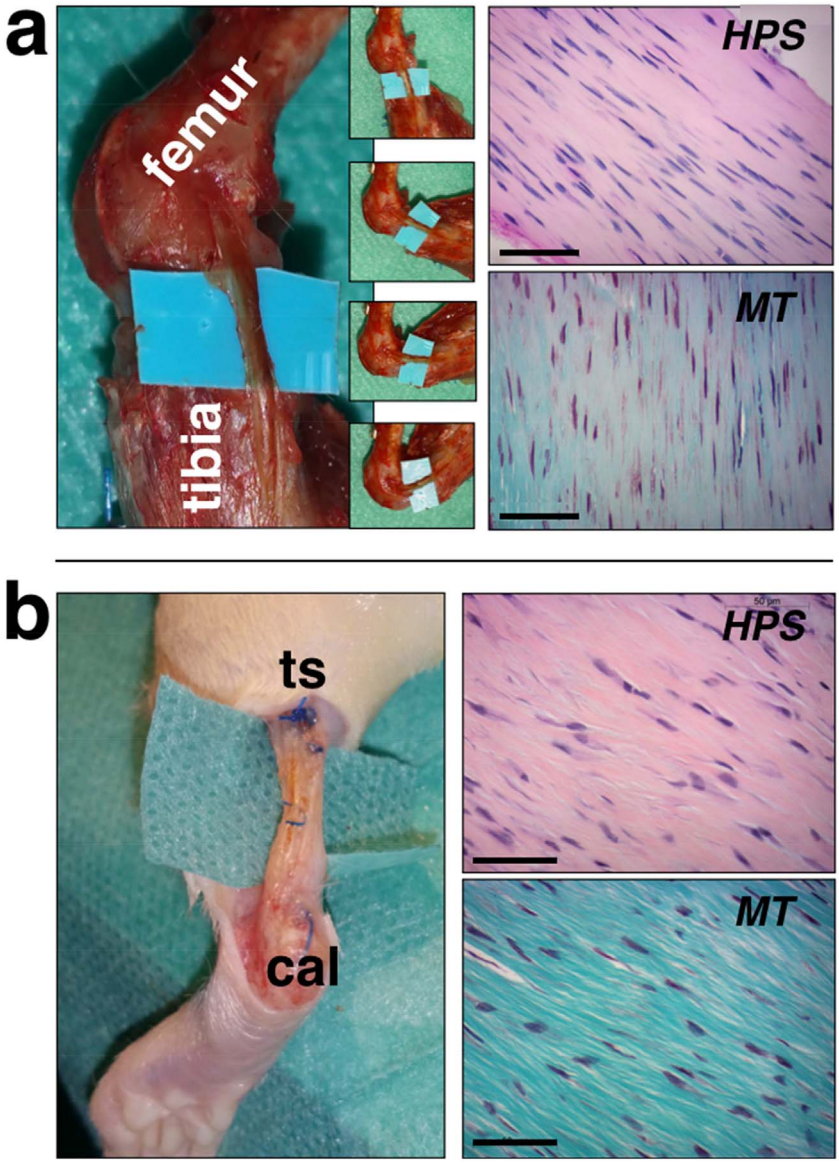

Fig. 6. Macroscopic views and histological analysis of the transplants six weeks after transfer for medial collateral ligament (a) and Achilles tendon (b) reconstruction.
cal: calcaneus; ts: triceps surae. Scale bar = 50 μm. HPS: Hematoxylin phloxine saffron and MT: Masson's trichrome.

matrix parallel to the loading axis (Doroski et al., 2010; Huisman et al., 2014; Yamamoto et al., 2003; Yamamoto et al., 2005). Moreover, Abousleiman et al. (2009) observed that in umbilical vein constructs seeded with MSCs, the application of cyclical longitudinal mechanical stimulations led to a differentiation of MSCs to tenocytes. They also found that the orientation of generated collagen bundles was parallel to the loading axis, while it was random without mechanical stimulation.

One puzzling element is that the silicone tube we implanted filled with a full cylindrical graft, while experiments using the Sparks' mandril method (which also uses a silicone tube) resulted in generation of hollow tubular grafts (Chen et al., 2013; Hallin and Sweetman, 1976). We believe that this is mainly due to the fact, in our study, the initial contents of the tube (a hematoma) was subjected to cyclical repetitive stresses. However, further experiments are required to elucidate the mechanisms involved.

Another important point to consider is the role of the holes in the PTI walls. Non-perforated PTI were empty, as no neo-tissue developed inside. In preliminary experiments (unpublished data), we observed that the number, size, and distribution of the holes influence the development of the neo-transplant. The presence of numerous vessels in the neo-tissue that developed into the holes (thereby connecting the neo-transplant and the neo-membrane surrounding the PTI) led us to hypothesize that these holes play a trophic role. Indeed, they permit blood supply to the growing neo-transplant that has important metabolic needs. Further experiments are now required to better understand the role of these holes and to optimize the design of the PTI.

This study presents some limitations. We implanted the PTI in the spine only for practical reasons, and the generated neo-tissue did not correspond to any existing ligament or tendon. We then used this neo-tissue as a transplant for reconstructive surgery in other joints, but we did not use the PTI to reconstruct a ligament or a tendon *in situ*. It would be interesting to analyze the feasibility of the direct implantation of a PTI to *in situ* regenerate a neo-tissue to replace a tendon or a ligament. Moreover, further experiments involving PTI with different geometries and mechanical properties will help to optimize its design and to better understand the mechanisms involved in the development of the neo-transplant.

We histologically examined for the presence of types I, II, and III collagens in the neo-transplant, but no analysis of other collagens or other components such as elastin and proteoglycans was performed at this stage. We observed a slight presence of type I collagen at 6 weeks, and we failed to identify the nature of the remaining collagen, while at 12 weeks, the neo-transplant mainly exhibited type III collagen bundles. Further studies are necessary to better analyze the structural

differences between the neo-transplant and ligaments and tendons, which are mainly composed of type I collagen (Rodrigues et al., 2013). In particular, we studied the generated tissue up to 12 weeks, but longer time points could be interesting to analyze the growth process.

We used young and growing rats, and as age can affect the healing capability of tissues, further experiments involving adult animals are necessary to confirm these first results. Finally, this PTI technique needs to be tested in big animals before any translation of the process to humans.

Despite these limitations, this study is a first step in the design and validation of a new strategy in bioengineering of using autologous transplants for ligament and tendon reconstructions.

5. Conclusion

The present study demonstrated the feasibility of an approach aiming to generate *de novo* and *in vivo* autologous transplants that can be used in ligament and tendon reconstructive surgery in rats. This approach only requires the implantation of a perforated tubular implant and no additional cells are necessary. The biomechanical properties of the generated transplants were consistent with those of native rat tendons and ligaments. However, before the translation of this technique to humans, further studies are required to better understand the mechanisms that lead to the generation and growth of the neo-transplant, to better characterize the structure of the generated tissue, and finally to optimize the implant design and the surgical technique.

Acknowledgement

The authors thank Olivier Thibaudeau (Department of histology, Universitary hospital of Bichat) for tissue processing and staining, the NOVOTEC company for immunohistochemical staining, Frederic Baudin and Ryma Nait (animal facility, Faculty of Medicine of Lariboisière, Paris) and Morad Bensidhoun (Osteo-articular bioengineering and bioimaging laboratory UMR7052, Faculty of Medicine of Lariboisière, Paris) for their cooperation in conducting this research.

This research did not receive any specific grant from funding agencies in the public, commercial, or not-for-profit sectors.

Conflicts of interest

None.

References

Abousleiman, R.I., Reyes, Y., McFetridge, P., Sikavitsas, V., 2008. The human umbilical vein: a novel scaffold for musculoskeletal soft tissue regeneration. Artif. Organs 32 (9), 735–742.

Abousleiman, R.I., Reyes, Y., McFetridge, P., Sikavitsas, V., 2009. Tendon tissue engineering using cell-seeded umbilical veins cultured in a mechanical stimulator. Tissue Eng. A 15 (4), 787–795.

Ahmed, A.S., Schizas, N., Li, J., Ahmed, M., Ostenson, C.G., Salo, P., Hewitt, C., Hart, D.A., Ackermann, P.W., 2012. Type 2 diabetes impairs tendon repair after injury in a rat model. J. Appl. Physiol. 113 (11), 1784–1791 (1985).

Altman, G.H., Horan, R.L., Martin, I., Farhadi, J., Stark, P.R., Volloch, V., Richmond, J.C., Vunjak-Novakovic, G., Kaplan, D.L., 2002. Cell differentiation by mechanical stress. FASEB J. 16 (2), 270–272.

Brunette, D.M., 1986. Fibroblasts on micromachined substrata orient hierarchically to grooves of different dimensions. Exp. Cell Res. 164 (1), 11–26.

Chen, J., Xu, J., Wang, A., Zheng, M., 2009. Scaffolds for tendon and ligament repair: review of the efficacy of commercial products. Expert Rev. Med. Devices 6 (1), 61–73.

Chen, X.S., Ou, T.W., Zhang, J., Li, J.X., Chen, B., Yu, H.X., Gu, Y.Q., Cui, Y.Q., Zhang, J.Y., Xu, Y.L., Sun, H.C., Liu, S., Wang, R., 2013. Histological and mechanical properties of autologous living tissue biotubes. Exp. Ther. Med. 5 (6), 1613–1618.

Cheng, C.W., Solorio, L.D., Alsberg, E., 2014. Decellularized tissue and cell-derived extracellular matrices as scaffolds for orthopaedic tissue engineering. Biotechnol. Adv. 32 (2), 462–484.

Christou, C., Oliver, R.A., Yu, Y., Walsh, W.R., 2014. The Masquelet technique for membrane induction and the healing of ovine critical sized segmental defects. PLoS One 9 (12), e114122.

Deranlot, J., Maurel, N., Diop, A., Pratlong, N., Roche, L., Tiemtore, R., Nourissat, G., 2014. Abrasive properties of braided polyblend sutures in cuff tendon repair: an in vitro biomechanical study exploring regular and tape sutures. Arthroscopy - Journal of Arthroscopic and Related Surgery 30 (12), 1569–1573.

Diop, A., Maurel, N., Chang, V.K., Kany, J., Duranthon, L.-D, Grimberg, J., 2011. Tendon fixation in arthroscopic latissimus dorsi transfer for irreparable posterosuperior cuff tears: an in vitro biomechanical comparison of interference screw and suture anchors. Clin. Biomech. 26 (9), 904–909.

Doroski, D.M., Levenston, M.E., Temenoff, J.S., 2010. Cyclic tensile culture promotes fibroblastic differentiation of marrow stromal cells encapsulated in poly(ethylene glycol)-based hydrogels. Tissue Eng. A 16 (11), 3457–3466.

Hallin, R.W., Sweetman, W.R., 1976. The Sparks' mandril graft. A seven year follow-up of mandril grafts placed by Charles H. Sparks and his associates. Am. J. Surg. 132 (2), 221–223.

Hothorn, T., Hornik, K., van de Wiel, M.A., Zeileis, A., 2008. Implementing a class of permutation tests: the coin package. J. Stat. Softw. 28 (8), 1–23.

Huisman, E., Lu, A., McCormack, R.G., Scott, A., 2014. Enhanced collagen type I synthesis by human tenocytes subjected to periodic in vitro mechanical stimulation. BMC Musculoskelet. Disord. 15, 386.

Issa, R.I., Engebretson, B., Rustom, L., McFetridge, P.S., Sikavitsas, V.I., 2011. The effect of cell seeding density on the cellular and mechanical properties of a mechanostimulated tissue-engineered tendon. Tissue Eng. A 17 (11 − 12), 1479–1487.

Kaux, J.F., Drion, P., Libertiaux, V., Colige, A., Hoffmann, A., Nusgens, B., Besancon, B., Forthomme, B., Le Goff, C., Franzen, R., Defraigne, J.O., Cescotto, S., Rickert, M., Crielaard, J.M., Croisier, J.L., 2013. Eccentric training improves tendon biomechanical properties: a rat model. J. Orthop. Res. 31 (1), 119–124.

Keller, B.V., Davis, M.L., Thompson, W.R., Dahners, L.E., Weinhold, P.S., 2013. Varying whole body vibration amplitude differentially affects tendon and ligament structural and material properties. J. Biomech. 46 (9), 1496–1500.

Mammoto, T., Seerattan, R.A., Paulson, K.D., Leonard, C.A., Bray, R.C., Salo, P.T., 2008. Nerve growth factor improves ligament healing. J. Orthop. Res. 26 (7), 957–964.

Mirzadeh, H., Shokrolahi, F., Daliri, M., 2003. Effect of silicon rubber crosslink density on fibroblast cell behavior in vitro. J. Biomed. Mater. Res. A 67 (3), 727–732.

Monteiro, J.C., Gomes, M.L., Tomiosso, T.C., Nakagaki, W.R., Sbervelheri, M.M., Ferrucci, D.L., Pimentel, E.R., Dolder, H., 2011. More resistant tendons obtained from the association of Heteropterys aphrodisiaca and endurance training. BMC Complement. Altern. Med. 11, 51.

Ng, K.W., Wanivenhaus, F., Chen, T., Abrams, V.D., Torzilli, P.A., Warren, R.F., Maher, S.A., 2013. Differential cross-linking and radio-protective effects of genipin on mature bovine and human patella tendons. Cell Tissue Bank. 14 (1), 21–32.

Nourissat, G., Diop, A., Maurel, N., Salvat, C., Dumont, S., Pigenet, A., Gosset, M., Houard, X., Berenbaum, F., 2010. Mesenchymal stem cell therapy regenerates the native bone-tendon junction after surgical repair in a degenerative rat model. PLoS One 5 (8), e12248.

Rodrigues, M.T., Reis, R.L., Gomes, M.E., 2013. Engineering tendon and ligament tissues: present developments towards successful clinical products. J. Tissue Eng. Regen. Med. 7 (9), 673–686.

Sharma, P., Maffulli, N., 2006. Biology of tendon injury: healing, modeling and remodeling. J. Musculoskelet. Neuronal Interact. 6 (2), 181–190.

Su, W.R., Chen, H.H., Luo, Z.P., 2008. Effect of cyclic stretching on the tensile properties of patellar tendon and medial collateral ligament in rat. Clin. Biomech. (Bristol, Avon) 23 (7), 911–917.

Suwalski, A., Dabboue, H., Delalande, A., Bensamoun, S.F., Canon, F., Midoux, P., Saillant, G., Klatzmann, D., Salvetat, J.P., Pichon, C., 2010. Accelerated Achilles tendon healing by PDGF gene delivery with mesoporous silica nanoparticles. Biomaterials 31 (19), 5237–5245.

Teramoto, A., Luo, Z.P., 2008. Temporary tendon strengthening by preconditioning. Clin. Biomech. (Bristol, Avon) 23 (5), 619–622.

Thorfinn, J., Angelidis, I.K., Gigliello, L., Pham, H.M., Lindsey, D., Chang, J., 2012. Bioreactor optimization of tissue engineered rabbit flexor tendons in vivo. J. Hand Surg. Eur. Vol. 37 (2), 109–114.

Vieira, C.P., De Oliveira, L.P., Da Re Guerra, F., Dos Santos De Almeida, M., Marcondes, M.C., Pimentel, E.R., 2015. Glycine improves biochemical and biomechanical properties following inflammation of the achilles tendon. Anat. Rec. (Hoboken) 298 (3), 538–545.

Yamamoto, E., Tokura, S., Hayashi, K., 2003. Effects of cyclic stress on the mechanical properties of cultured collagen fascicles from the rabbit patellar tendon. J. Biomech. Eng. 125 (6), 893–901.

Yamamoto, E., Kogawa, D., Tokura, S., Hayashi, K., 2005. Effects of the frequency and duration of cyclic stress on the mechanical properties of cultured collagen fascicles from the rabbit patellar tendon. J. Biomech. Eng. 127 (7), 1168–1175.

Yang, G., Rothrauff, B.B., Tuan, R.S., 2013. Tendon and ligament regeneration and repair: clinical relevance and developmental paradigm. Birth Defects Research Part C - Embryo Today: Reviews 99 (3), 203–222.